



Manufacturing Space Homogeneity in Additive Manufacturing – Electron Beam Melting Case

Alexandre Piaget, Matthieu Museau, Henri Paris

► To cite this version:

Alexandre Piaget, Matthieu Museau, Henri Paris. Manufacturing Space Homogeneity in Additive Manufacturing – Electron Beam Melting Case. MIT Conference, Laboratory for Alternative Technologies, Uni. of Ljubjana, Slovenia, Sep 2016, Fiesa, Slovenia. hal-01390804

HAL Id: hal-01390804

<https://hal.science/hal-01390804>

Submitted on 2 Nov 2016

HAL is a multi-disciplinary open access archive for the deposit and dissemination of scientific research documents, whether they are published or not. The documents may come from teaching and research institutions in France or abroad, or from public or private research centers.

L'archive ouverte pluridisciplinaire **HAL**, est destinée au dépôt et à la diffusion de documents scientifiques de niveau recherche, publiés ou non, émanant des établissements d'enseignement et de recherche français ou étrangers, des laboratoires publics ou privés.

Manufacturing Space Homogeneity in Additive Manufacturing – Electron Beam Melting Case

A. Piaget, M. Museau and H. Paris

Univ. Grenoble Alpes, CNRS, G-SCOP, 38 000 Grenoble, France

Abstract

This paper focuses on the homogeneity of the manufacturing space of the EBM (Electron Beam Melting) technology. An Arcam AB A1 machine is used as tool for experimentations, with titanium (Ti-6Al-4V) as material. The objective of this study is to show the correlation between workpieces geometrical deformations and their position in the manufacturing space. Results show that the position on Z-axis does not affect quality, but there is a strong link in the Z-plane: significant defects appear near the manufacturing space boundaries. First manufactured layers are deformed in the vicinities of the manufacturing space edges. Up to 3mm of material loss and 8mm of dimensional deformation are measured. Further analyses point that this phenomenon is particularly related to a sintering variation in the powder: there are up to 3% density difference from the centre to borders. To avoid the problem, reduction of the manufacturing space and a supporting strategy are proposed. Defects can also be removed by implementing thermal insulation on the machine or by modifying the beam operation.

Keywords: Quality Management, Additive Manufacturing, Electron Beam Melting, Manufacturing Space Homogeneity.

1 Introduction

The additive manufacturing technologies have become essential tools for modern industry [1][2]. Among the different additive manufacturing technologies, EBM (Electron Beam Melting) is able to manufacture a wide range of metallic parts (massive, topologically optimized, lattice structure) [3] [4]. Compared to SLM (Selective Laser Melting), the EBM technology is still poorly studied [5]. However, there is a strong need to further master this technology. Aeronautic, spatial and also medical fields are particularly interested in mastering the quality provided by this process [6][7][8][9].

In order to control the quality, without destruction of manufactured parts, test specimens are manufactured simultaneously [10]. By testing those specimens, information about the quality of manufactured parts is obtained. Most of the time, specimens are arranged in the edges of the manufacturing space. A question arises about the homogeneity of the manufacturing space. Indeed, heterogeneity could lead to errors in the manufacturing and control processes. This key point that is not addressed in the literature, is the topic of this paper.

The problem is approached by studying the geometrical deformation which is the main defect. Previously, several parts showed defects when they were manufactured within certain areas of the manufacturing space. Thus, there is a need to characterise this space and its heterogeneity, and the way it impacts on the manufactured parts. These characteristics are related to the machine used (described below), but the experimental method can be applied to other machines.

In the next part, the context of the study and the experimentation are exposed. The type of deformation and measures are presented. Secondly, the possible sources of this defect are analyzed. We also show the impact they may have on manufactured parts. Finally we conclude about the dangers of this phenomenon and the prospects for resolution.

2 Defect identification

2.1 Context

The Arcam AB A1 machine [11] [12] uses an electron beam to melt powder (Figure 1). The powder from the hoppers is spread over a platform in 50µm thick layers with a rake. The electron beam sinters the whole of

the introduced powder. This increases the thermal and electrical conductivity. Then it locally melts the powder to manufacture the desired geometry. The platform finally goes down of the thickness of a layer and this cycle can be repeated.

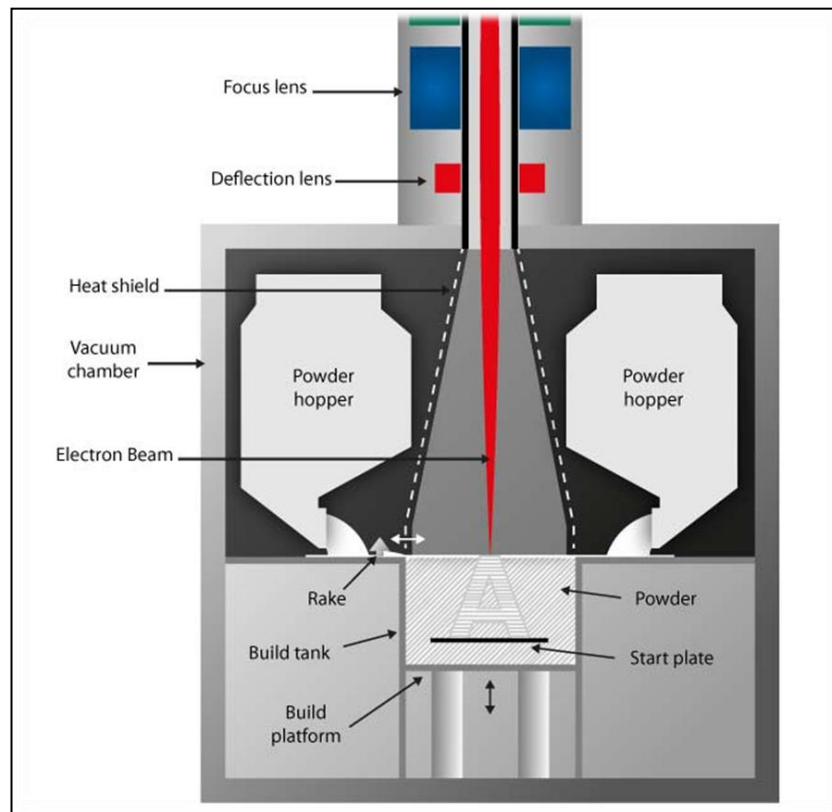


Figure 1: Arcam EBM systems, schematic architecture [11]

In order to qualify the geometric defect, some parameters have to be chosen. Ti-6Al-4V powder from Arcam AB is used for the study. Vayre [13] shown that Arcam AB standard parameter set is well balanced for printing several kind of geometry (lattice structures, massive workpieces...) at the same time. Thereby, this parameter set¹ is kept for the whole experimentation. Otherwise, workpieces will be built without any supporting strategy. Indeed, EBM technology doesn't necessarily involve a supporting strategy to build workpieces [14]. Based on Vayre [15], there is no need to add support to the experimental workpieces (described in the section below) because of the experimented workpieces thinness. Hereafter, evidence that supports aren't necessary to manufacture these workpieces is provided.

For the experimentation, the largest manufacturing space available with the machine is needed. But the manufacturing space is limited by the use of software² that reduce the initial manufacturing space (200*200*180) to 195mm in length, 195 in width and 180 in height.

2.2 Experimentation

The first objective of this study is to evaluate the impact of the position in the manufacturing space on the final workpiece geometry. Indeed, deformations are observed on several workpieces made by EBM. In order to show and identify this phenomenon, the following experimentation is realized.

The principle is to build one workpiece at different locations in the manufacturing space. Then, differences and defects can be observed and correlated to the location. Two kinds of workpieces have been selected for the test (Figure 2). The first one is a massive workpiece. The second one is a lattice structure. Thus, those workpieces represent the two kinds of geometry cases encountered.

¹ Arcam theme melt 50μm for TA6V

² Magics (Materialise), Build Assembler (Arcam AB)

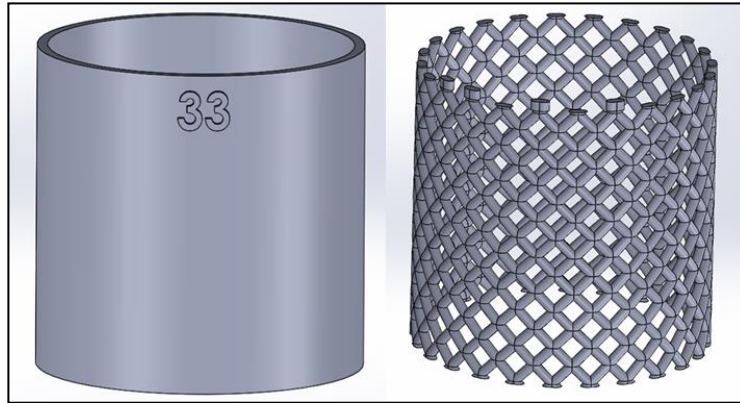


Figure 2: Experimentation workpieces, massive (left) and lattice structure (right).

The height and the diameter of the pipes are 30mm. The thickness of the wall for the massive pipe and of the beam for the lattice one is 1mm. Inside each pipe, two other pipes with different diameters ($\varnothing 20\text{mm}$ and $\varnothing 10\text{mm}$) are integrated to the experimentation in order to have different thermal conditions. Indeed, the $\varnothing 10\text{mm}$ workpiece always has a $\varnothing 20\text{mm}$ and a $\varnothing 30\text{mm}$ pipes for neighbours while the $\varnothing 30\text{mm}$ workpiece has a number of neighbours depending on its position.

The experimentation consists in testing 25 locations of the manufacturing space. Grouped by three, workpieces will be repeated on each locations of a unique altitude of the manufacturing space in order to avoid scan length problems [16]. By measuring each workpieces, defects are characterized and linked to the location.

Observations show that the defect appears in first layers. Therefore, the lower part of the workpieces is analysed and that is the reason why the workpieces are represented upside down later in the document. The measurement protocol for the massive workpiece uses a three-dimensional optical control machine³ in order to measure deformation on the first manufactured layer. This layer is controlled at 24 points (every 15 degrees) distributed all along the surface. The result of a measure is the height of the controlled point with a $2\mu\text{m}$ precision. From this, we recovered the difference between the nominal height and the measured one (Figure 3, left).

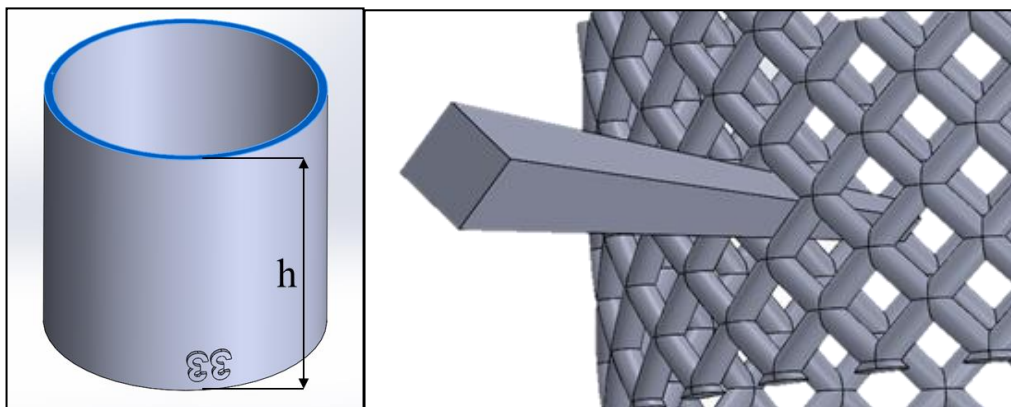


Figure 3: Representation of the measurement processes: massive (left) and lattice (right) workpieces

Measuring the first layer deformation does not provide information on the deformation of the following layers. With the lattice structure, the target is to measure the defect spread through several layers. Consequently, the measurement protocol has to be adapted. A tool has been created to control the external geometry of the lattice pipe (Figure 3, right). This way, we may have information about the defect on the pipe: its angular position and altitude.

³ Used machine : Vertex, <https://www.microvu.com/>

2.3 Results

Measures are presented in a radar chart in order to represent the size and the angular position of the defect. So, in the diagrams, the more a point is far from the middle, the more the defect is important. As shown in Figure 4, defect occurs on some workpieces (on both pictures, the left workpiece fits the CAD model and the right includes a deviation from the model). The defect is materialized in two forms: material loss and geometric deformation. Lattice structures show both failure (Figure 4): between the well-shaped and the defective workpiece, deformations are observed in first layers (missing) and in diamond meshes (misshapen).

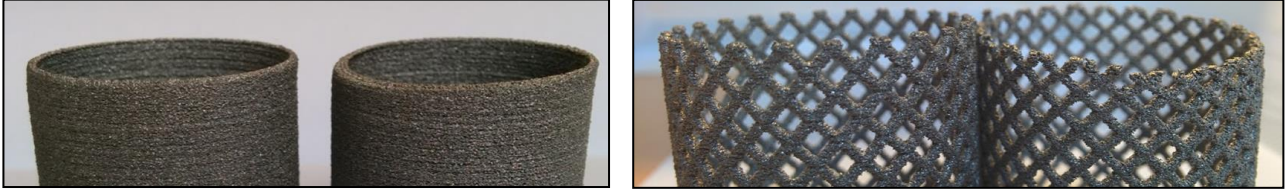


Figure 4: massive (left) and lattice (right) workpieces placed upside down

Figure 5 presents the results for the massive workpiece. From these results, occurrences of defects on nearby workpieces of borders are observed. Furthermore, the defect is more critical as the point observed on a workpiece is close to the borders. The biggest gap measured between the nominal and the manufactured surface is 3mm high. Whereas, for the inner workpieces, measured defects are smaller than 0.8mm. But this fact corresponds with the 50 μ m roughness owned by the material resource [16].

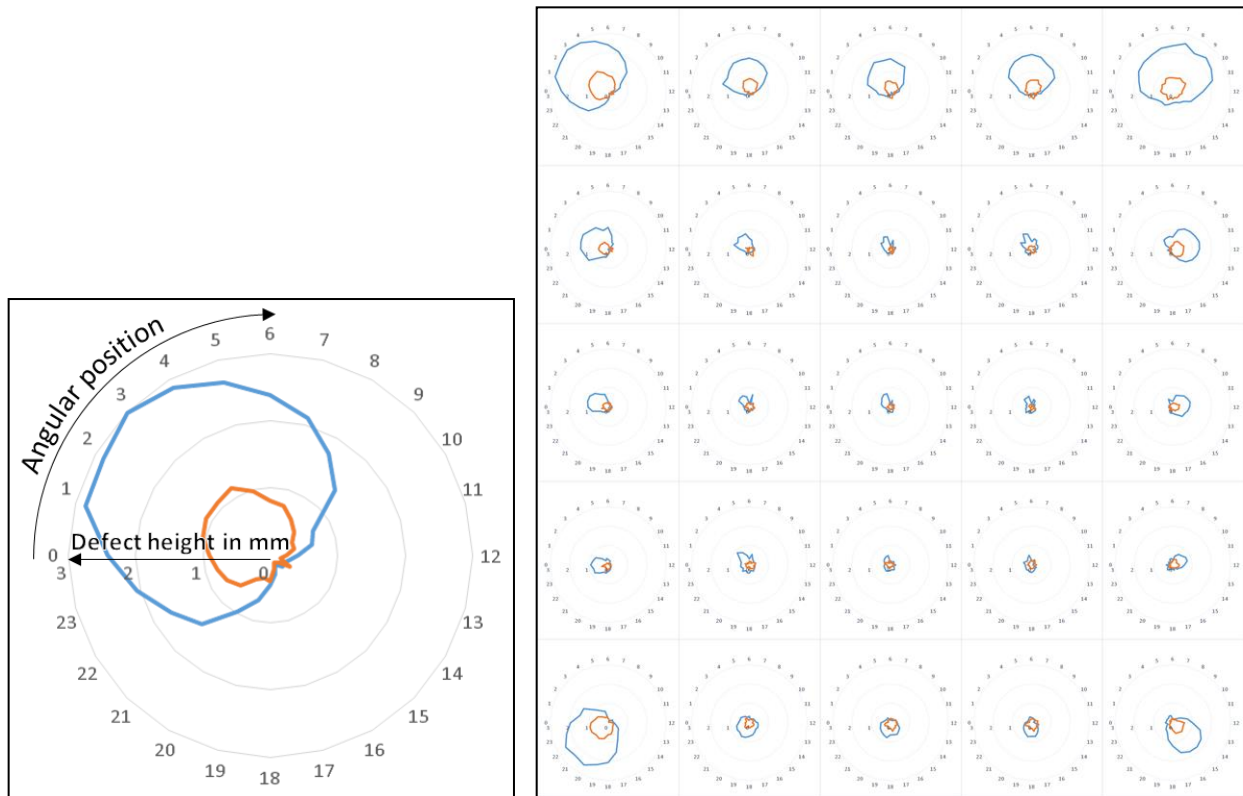


Figure 5: Example and defect cartography of the massive workpieces (blue: Ø30mm, orange: Ø20mm).

Figure 6 presents results for the lattice workpieces in numbers of defective cells, for an angular position and starting from the bottom of a workpiece. The same conclusion can be drawn as there is no defect in the inner workpieces and the external workpieces have an outwardly directed defect. In addition, the highest measured defect is 8mm high from the first layer.

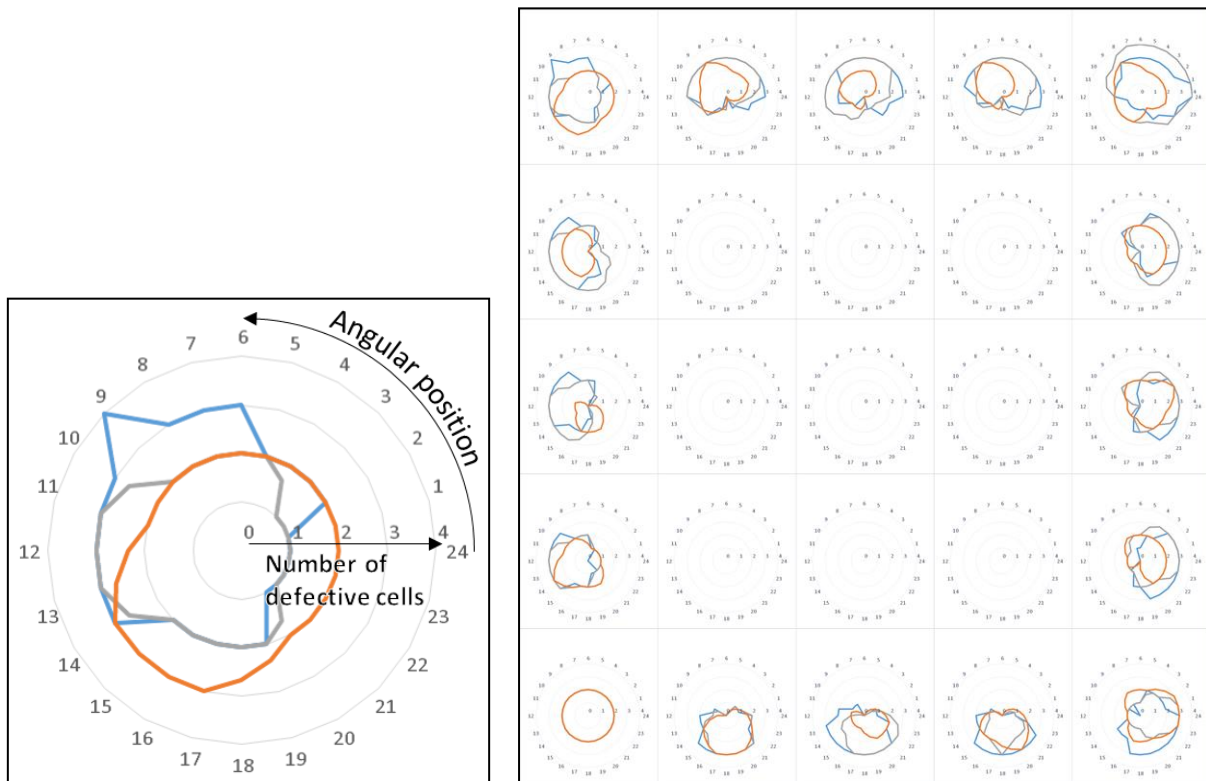


Figure 6: Example and defect cartography of the lattice workpieces (blue: 30mm, orange: 20mm, grey: 10mm).

Another interesting point is that a group of workpieces (located at the bottom right in Figure 6) has undergone a 2mm mechanical shifting. The 3 curves are overlapping because workpieces cells are all affected in the same way. What is interesting in this point is that it brings other elements to explain and understand the sources and consequences of the deformation phenomenon, although this shifting is not repeatable. Figure 7 is a photography that shows the encountered problem. This shifting is in the movement direction of the rake.

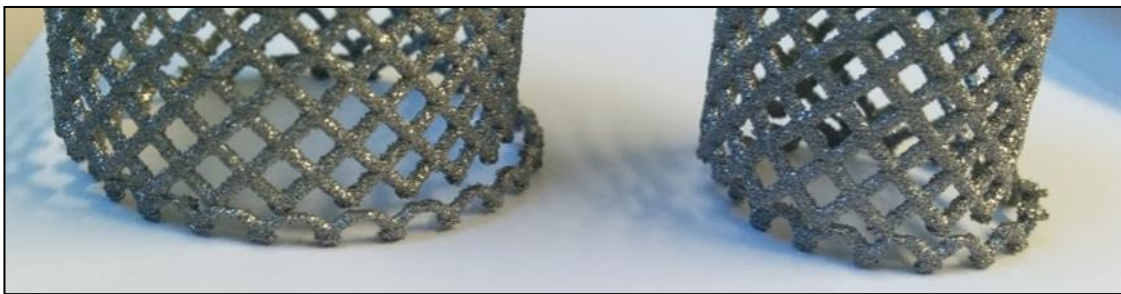


Figure 7: Photography of the 2mm mechanical shifting (Ø30mm on left, Ø20mm on right).

Finally, observations and measures show that only the workpieces near the borders of the manufacturing space are reached by the defects. In corners, the defect reaches its highest value: the maximal height of the defect is 8mm from the first layer. Those defects are significant enough to justify a thorough study with the aim to master and avoid this problem.

3 Phenomenon Analysis

3.1 Hypothesis

To explain the phenomenon, several hypotheses have been expressed. First, the electron beam hypothesis has been selected. Indeed, to reach borders, the electron beam has to undergo an important deflection that leads to change the shape of the beam from a circle to an ellipse. The energy broadcasted to the powder is lower as

the surface of transmission gets bigger. It generates a decrease in the temperature that prevents the melting of the powder. This decrease might explain the location of the defect and the defect type also.

The second hypothesis concerns the workspace in the machine. At the borders of the manufacturing space, next to the sintered powder, there are cold powder and the metal enclosure that might absorb the energy of the sintered powder and thereby generate a loss of temperature. As TA6V is a bad thermal conductor [8], this phenomenon might just take place at the border between the sintered powder and the cold powder. Lowering temperature locally leads to the same conclusion as the electron beam hypothesis.

A third hypothesis arises from the mechanical shifting (Figure 7). As a portion of the workpiece has been moved in the rake direction, this hypothesis involves the rake: when the rake spreads the powder out, it can move the matter underneath by the thrust applied on the powders. That might cause deformation and matter loss in the workpiece.

The first and the second hypothesis might explain the difference between the workpieces but they don't solve the matter shifting. On its side, the third hypothesis elucidates the shifting but there is no reason for the non-homogeneity of that phenomenon.

The hypothesis we kept is a combination of the previous ones: the contact area of the electron beam is circular in the powder bed center, but away from the center, it becomes elliptical and provides less energy to the powder. In addition, the energy leaks with the proximity to cold powders and metal enclosure. This makes the sintering of the powder weaker near the borders. Then, the rake passage might easily move the poorly sintered powder and the molten material suspended in the powder. This might lead to a loss of material as well as deformation for the manufactured parts. In addition, the sintering weakness modifies the thermal conductivity, the cooling of the manufactured parts is no more homogeneous and it generates additional deformation.

3.2 Analysis

In order to validate the hypothesis, an analysis of the sintered powder is made. This analyse was conducted with an X-ray microtomography machine. The machine is able to reconstruct a 3D model of the studied sample with voxels. This reconstruction aims to display and measure the size of the necks binding in the sintered powder. A difference of necks size between the powders in the centre and in the periphery of the manufacturing space would indicate a significant difference of the sintering [19].

The samples of powders are one centimetre side cube. This size allows observation of a large number of powder grain that limits the impact of defects in the powder. Due to the titanium opacity to X-ray, getting a 1 μ m resolution with titanium parts requires more power than supplied by the machine [18]. Resolution has been reduced to 5 μ m in order to provide a clear tomography of the samples. Despite a clear tomography, it becomes impossible to measure necks because of the resolution. However, [19] show there is a link between density and sintering progress with spherical powders. Thereby, measuring density permits comparison of the two samples sintering.

Table 1: Porosity measured from the tomography reconstruction

Samples	Centre	Periphery
Porosity (%)	37.84	41.29
Standard Deviation (%)	1.36	1.92

Table 1 presents the results of the analysis. With more than 3% difference, assumptions about the difference of sintering are justified. Indeed, according to OLMOS [19], 3% are significant enough to make a difference of sintering. This difference impacts the powder stiffness and its heat conductivity. This generates a harmful heterogeneity in the manufacturing space that might have bad effects on manufactured parts [20].

4 Conclusion

The observed defect has an impact on geometry of manufactured parts with EBM technology. According to their position, parts may undergo geometric deformation and matter loss. It can be inferred from this study that the manufacturing space is heterogeneous.

In the worst case, the 8 first millimeters are affected by this defect. The closest defect to the center is 86mm distant from the center. The more the defect is far from the center, the more important it is. With this information, a first strategy can be used to bypass the defect. Indeed, creating supports 8mm (or more) long all along the first layer permits to transfer the defect from the part to supports. A manufacturing space reduction to an 86mm radius cylinder can also be a solution to avoid the defect apparition. Those 2 strategies have been validated with the workpieces.

As well, modification could be made to change the machine operation and more precisely the electron beam. By bringing more energy, the powder sintering would be homogenized. Improve the insulation of the powder bath with the machine will also limit the energy loss.

References

- [1] I. Gibson, D. Rosen, B. Stucker: Development of Additive Manufacturing Technology. Additive Manufacturing Technologies, pp 19-42, 2015.
- [2] W. Gao, Y. Zhang, D. Ramanujan, K. Ramani, Y. Chen, C. B. Williams, C. C. L. Wang, Y. C. Shin, S. Zhang, P. D. Zavattieri: The Status, Challenges, and Future of Additive Manufacturing in Engineering. Computer-Aided Design 69, pp 65-89, 2015
- [3] N. Hrahe, and T. Quinn: Effects of Processing on Microstructure and Mechanical Properties of a Titanium Alloy (Ti-6Al-4V) Fabricated Using Electron Beam Melting (EBM). Materials Science and Engineering: A, V. 573, 20 June 2013.
- [4] N. Novak, M. Vesenjak, Z. Ren: Auxetic Cellular Materials – a Review. Journal of Mechanical Engineering 62, pp 485-493, 2016.
- [5] S.L. Sing, J. An, W. Y. Yeong, and F. E. Wiria: Laser and Electron-Beam Powder-Bed Additive Manufacturing of Metallic Implants: A Review on Processes, Materials and Designs. Journal of Orthopaedic Research, October 2015.
- [6] S. Daneshmand, C. Aghanajafi: Description and Modeling of the Additive Manufacturing Technology for Aerodynamic Coefficients Measurement. Journal of Mechanical Engineering 58, pp 125-133, 2012.
- [7] J. M. Waller, B. H. Parker, K. L. Hodges, E. R. Burke, and J. L. Walker: Nondestructive Evaluation of Additive Manufacturing. National Aeronautics and Space Administration, November 2014.
- [8] G. Budzik, J. Burek, A. Bazan, P. Turek: Analysis of the Accuracy of Reconstructed Two Teeth Models Manufactured Using the 3DP and FDM Technologies. Journal of Mechanical Engineering 62, pp 11-20, 2016
- [9] V. Petrovic, J. V. Haro, J. R. Blasco, and L. Portolés: Additive Manufacturing Solutions for Improved Medical Implants. Metal-Processing Research Institute AIMME, Valencia, Spain, 2012.
- [10] CCT MAT – STR, CNES: PRINTtemps de la Fabrication Additive. Toulouse, June 2016
- [11] Arcam AB: Creating New Opportunitites in Design and Production. www.arcam.com/wp-content/uploads/justaddbrochure-web.pdf, 2016
- [12] Arcam AB: Arcam A1, the Future in Implant Manufacturing. <http://www.arcam.com/wp-content/uploads/Arcam-A1.pdf>, 2010
- [13] B. Vayre: Conception pour la Fabrication Additive, Application à la Technologie EBM. PhD Thesis, Univ. Grenoble Alpes, 2014.
- [14] A-F. Obaton, A. Bernard, G. Taillandier, J-M. Moschetta: Fabrication additive: Etat de l'Art et Besoins Métrologiques Engendrés. Rev. Franç. Métr. N°41, 2016.

- [15] B. Vayre, F. Vignat, and F. Villeneuve: Identification on Some Design Key Parameters for Additive Manufacturing: Application on Electron Beam Melting. *Procedia CIRP* 7, pp. 264 – 269, 2013
- [16] A. Safdar: A study on Electron Beam Melted Ti-6Al-4V. Lund University, 2012.
<http://lup.lub.lu.se/record/2543181>, accessed august 2016.
- [17] J. A. Slotwinski, E. J. Garboczi, P. E. Stutzman, C. F. Ferraris, S. S. Watson, and M. A. Peltz: Characterization of Metal Powders Used for Additive Manufacturing. *Journal of Research of the National Institute of Standards and Technology*, Volume 119, 2014.
- [18] C. Thiery: Tomographie à Rayons X. *Techniques de l'Ingénieur*, 10 December 2013.
- [19] L. Olmos: Etude du Frittage de Poudres par Microtomographie in situ et Modélisation Discrète. PhD Thesis. Institut National Polytechnique de Grenoble - INPG, 2009.
- [20] C.-M. Zou, Y. Liu, X. Yang, H-W. Wang, and Z-J. Wei: Effect of Sintering Neck on Compressive Mechanical Properties of Porous Titanium. *Transactions of Nonferrous Metals Society of China*, Volume 22, Supplement 2, December 2012, Pages s485-s490.